24th COBEM - 2017

24th ABCM International Congress of Mechanical Engineering
December 3-8, 2017, Curitiba, PR, Brazil

COBEM-2017-2656
ANALYSIS OF THE EFFECT OF SPOT WELDING CURRENT ON THE MECHANICAL BEHAVIOR AND FAILURE MODES OF AUTOMOTIVE STEEL SHEETS

Tiago Cristofer Aguzzoli Colombo
Fábio do Monte Sena
José Jerônimo Rabelo Faria
Alfredo Rocha de Faria
Instituto Tecnológico de Aeronáutica. Department of Aeronautical and Mechanical Engineering. São José dos Campos, SP, Brazil.
colombo@ita.br, sena@ita.br, jfaria@ita.br, arfaria@ita.br

Abstract. *The present paper aims to study the influence of the weld current on the mechanical performance of low-C Al-killed drawing quality (AKDQ) steel samples welded through Resistance Spot Welding (RSW). The samples were subjected to quasi-static tensile-shear tests and results were used to assess the load-bearing capacity and energy absorption for different weld current conditions. Additionally, nugget size, indentation depth and hardness parameters were also assessed for all samples. Results indicate that for the evaluated weld currents there is a clear optimum process window for automotive applications, ranging from 12kA to 16kA. Transition in failure mode was observed at 10kA, at which the predominant mode becomes pullout, promoting high energy absorption and mechanical strength. Moreover, for weld currents higher than 17kA a considerable decrease in mechanical performance was observed.*

Keywords: *Resistance Spot Welding, Automotive Manufacturing, Automotive Steels*

1. INTRODUCTION

Among the manufacturing processes applied to automobile assembly, Resistance Spot Welding (RSW) is considered the most important joining method due to its high production efficiency, low cost, as well as ease of operation and automation when compared to other assembly processes. The quality of the spot welds has significant influence on the structural integrity and reliability of the vehicle and consequently in passenger safety (Wan, 2014; Runnemalm, 2014). In a typical private passenger vehicle, there are about 5000 spot welds (Nick Johannes Den Uijl, 2015). The considerable number of spot welds is strongly influenced by the difficulty to evaluate spot weld quality, which is overcame by redundancy (re-spot). On the other hand, the highly competitive automobile industry demands a constant decrease in production costs and increase in process efficiency, driving the reduction of the number of spot welds, what may directly affect safety and performance of automotive structures. Therefore, there is a large technological importance for car makers in better understanding how RSW parameters may affect mechanical performance, failure modes and the quality of the spot welds. Any optimization in this manufacturing process has the potential to generate productivity gains on the shop floor and improvement in the quality of spot welds, consequently increasing the safety of automotive structures (Kianersi, Mostafaei and Ali, 2014; Martín *et al.*, 2014).

In the light of the above, the aim of this work is to investigate the effect of the spot welding current on the mechanical performance of spot welds performed on low-C Al-killed drawing quality (AKDQ) steel, widely applied in body-in-white manufacturing. Aspects associated with the quality of spot welds are taken into account, such as electrode indentation depth, spot weld dimensions and molten expulsion, in order to determine the optimum process window for the referenced material.

2. EXPERIMENTAL PROCEDURES

Al-killed drawing quality (AKDQ) (eq. AISI 1018) galvanized steel sheets, with a thickness of 0.7 mm and chemical composition given in Table 1, were used as the Base Material (BM). The steel sheets, as received in cold rolled condition by a domestic steel manufacturer, were cut in 50 × 30 mm rectangles and welded by RSW, adopting linear overlapping of the steel sheets, according to Figure 1. Welding was conducted using a Düring CB 150/560/76 kvA spot welding machine, with manual clamp, a Harms & Wende Ratia 73 controller and copper electrodes with a face diameter of

6.0 mm, equipped with a water cooling system. In order to investigate the influence of heat input on mechanical properties and metallurgical microstructure characteristics, the welding currents were selected from 7 to 18 kA with an increment of 1 kA. All other parameters were kept constant, as shown in Table 2.

Quasi-static tensile-shear tests were performed using an Instron 5500R/4206 Universal Testing Machine at a cross head displacement rate of 5 mm.min-1, according to the AWS/SAE/D8.9 standard (AWS, 2012). Mechanical strength of the spot welds was investigated and compared for each welding current interval by analyzing the load-displacement curves obtained from tensile tests up to the maximum tensile-shear load. Ten specimens were tested for each welding current condition. The Amount of Energy Absorption (AEA) was calculated by numerically integrating the area under the load-displacement curve up to the maximum load.

Table 1. Chemical composition and mechanical properties of the base material.

Chemical composition (%wt.)				Mechanical Properties		
C (max)	Mn (max)	P (max)	S (max)	Yield Strength (MPa)	Ultimate Tensile Strength (MPa)	Elongation (%)
0.12	0.60	0.05	0.05	140 (min.)	280 (min.)	30 (min.)

Table 2. Welding parameters.

Parameter	Magnitude
Squeeze time	32 cycles
Welding time	7 cycles
Holding time	12 cycles
Electrode force	200 kgf
Sheet thickness	0.7 mm

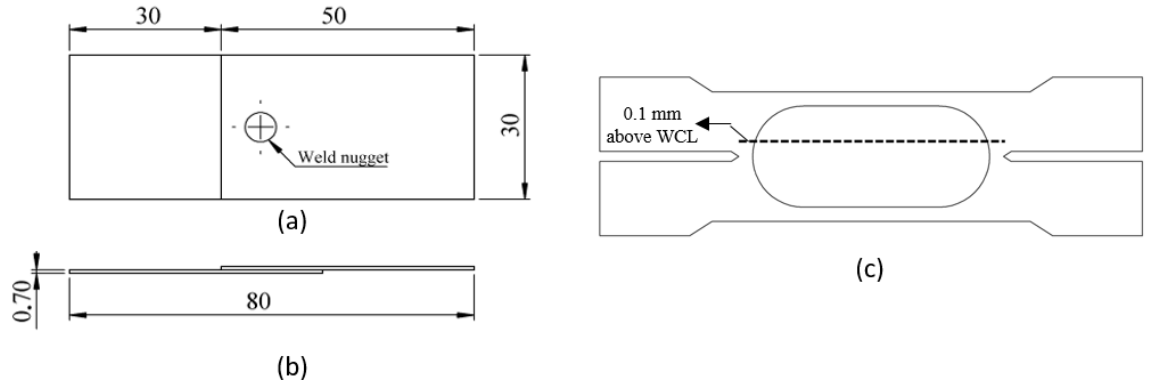

Figure 1. Schematic view of the spot weld samples: (a) superior view, (b) front view and (c) cross section view of the spot weld indicating where the hardness profiles were taken. Dimensions in mm.

The spot weld size of the tested samples was measured through a chisel test, where the spot weld is detached with the aid of a hammer and chisel, exposing the Fusion Zone (FZ) for measurement. This measurement method is widely employed in the industry, and it is standardized by ISO 10447 (ISO, 2006). For each current level, all ten specimens were measured and the mean spot weld size calculated. Vickers microindentations were performed on metallographic samples across the FZ, Heat Affected Zone (HAZ) and BM, at a distance of 0.1 mm above the Weld Centerline (WCL), as shown in Fig. 1 (c). The indentations were performed with a load of 1 N for 5s, with a spacing of 0.3 mm between each indentation, according to ASTM E384 (ASTM International, 2016). Moreover, the indentation caused by electrode penetration was measured using a Cyber CT-100 non-contact profilometer.

3. RESULTS AND DISCUSSIONS

3.1 Mechanical Performance and Failure Modes

Fig. 2 (a) shows the influence of welding current on spot weld size. Mechanical behavior and failure mode of spot welds are strongly affected by the spot weld size and thus the nugget size (Pouranvari *et al.*, 2011). According to Pouranvari *et al*. (Pouranvari *et al.*, 2007), the change in electrical resistance of the steel sheet has a strong influence on the growth rate of the nugget. At the beginning of the welding process, the increase in temperature of the sheet metal

causes a proportional increase in electrical resistance, which in turn promotes a pronounced effect on nugget size growth. For AKDQ steel, this rapid weld size growth period occurs up to 11 kA, as shown in Fig. 2 (b). As the nugget size increases, dynamic resistance tends to decrease, causing a reduction on the growth rate, which occurs between 12 kA and 15 kA. Above 15 kA, a steady state is reached, where the competition between spot size growth, due to an increase in welding current, and the reduction of the molten metal volume, due to molten expulsion, causes a stabilization of the spot weld size, with no size growth with further increase in welding current (Pouranvari *et al.*, 2007). Therefore, for spot welds with current level equal to 15 kA and above, the spot weld size tends to stabilize around 6.5 mm, which is slightly above the diameter of the electrode tips.

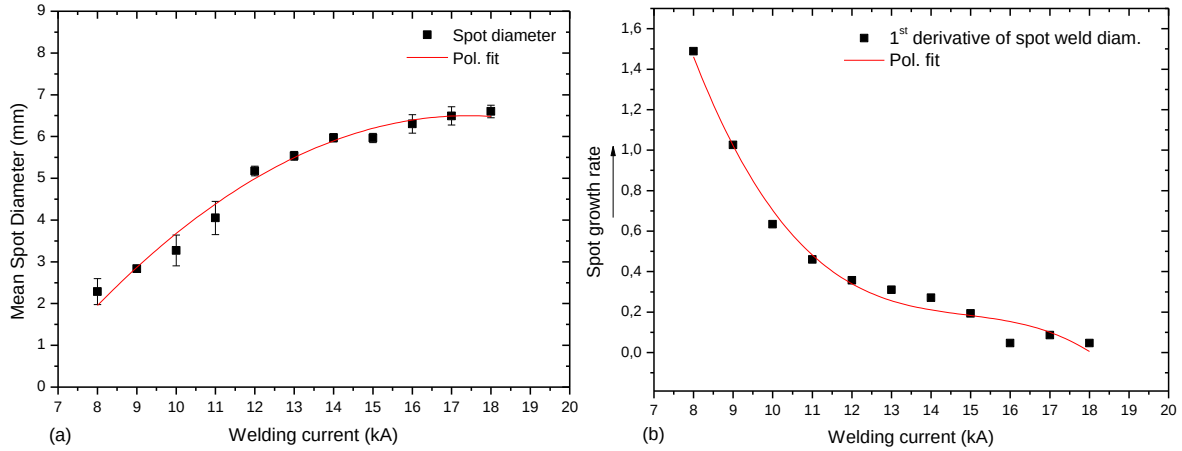

Figure 2. Influence of the welding current on: (a) spot weld size and (b) spot weld growth rate.

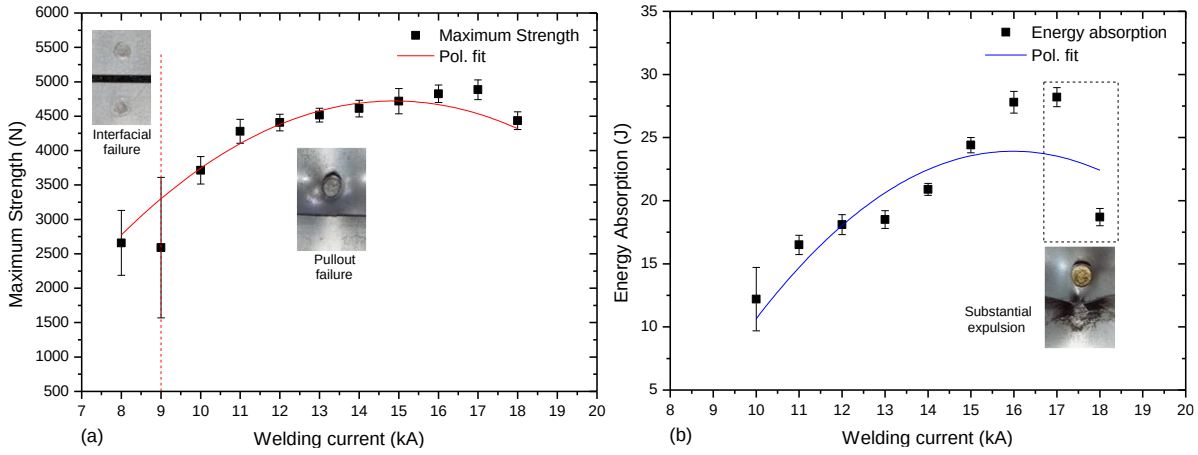

Figure 3. Mechanical properties as a function of welding current: (a) maximum tensile-shear load and (b) energy absorption at the maximum load.

In this work, mechanical properties were described in terms of the maximum load that the spot weld can withstand, and energy absorption capability, determined by the area under the load-elongation curve up to the maximum load. These are two important properties that can be directly correlated with spot weld quality. Literature suggests that the load-bearing capacity and the energy absorption capability follow the same tendency of the spot weld size, increasing with an increase in welding current (Pouranvari and Marashi, 2011; Pouranvari *et al.*, 2011; Liu *et al.*, 2012). It can be seen from Fig. 3 (a) and (b) that both the load-bearing capacity and the energy absorption of the spot welds increase with increasing welding current up to 17 kA, then start to decrease. An abrupt decrease in energy absorption is observed for a welding current of 18 kA, indicating the degradation of the mechanical properties with further increase in welding current. These results suggest that mechanical strength cannot be considered directly dependent solely on spot weld size.

The decrease in mechanical strength and energy absorption above 17 kA can be attributed to different factors, especially excessive molten expulsion and electrode indentation (Kianersi, Mostafaei and Ali, 2014). Indentation, or electrode penetration depth, occurs due to an increase in sheet temperature during the welding process, followed by a decrease in mechanical strength. This decrease in mechanical strength, combined with a constant force acting on the sheet surface during welding, leads to the penetration of the electrode tips on the steel sheet, which in turn may lead to a decrease

in the load-bearing capacity of the joint. Shop floor practices in the automotive industry and literature recommend a maximum indentation of 20% of the workpiece thickness (Sun *et al.*, 2007).

Fig.4 shows the change in indentation as a function of welding current. It is evident a pronounced increase in indentation as welding current increases, especially for welding currents above 11 kA. Taking into account the aforementioned recommendation of a maximum indentation of 20% of the workpiece thickness, which corresponds to 280 µm, the maximum welding current to be applied should be 13 kA. This is a somewhat conservative value, since the load-bearing and energy absorption capacities can be further increased for higher current levels, up to 17 kA. At such current level, the indentation depth is approximately 620 µm, or 44%.

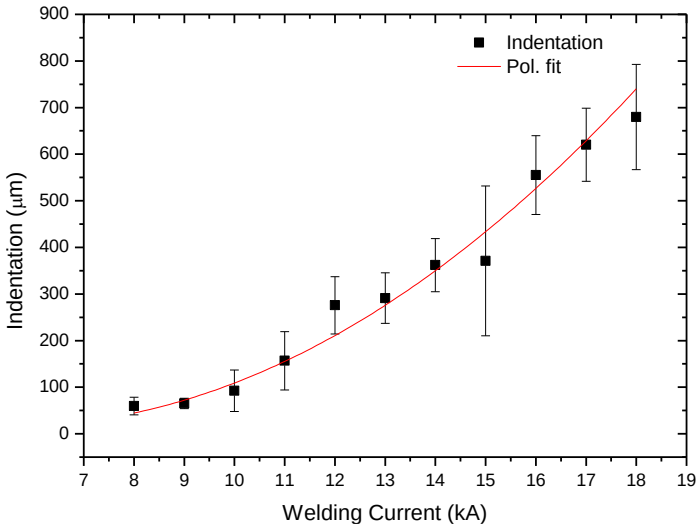

Figure 4. Indentation of electrode on workpiece as a function of welding current.

3.2 Failure Investigation

As aforementioned, impact absorbed energy is a critical property to ensure collision safety of motor vehicles, and is believed to have a direct correlation with the failure mode of spot welds (Sun, Stephens and Khaleel, 2008; Kong *et al.*, 2014). Generally, the spot weld failure occurs in three modes: Interfacial Failure (IF), Pullout Failure (PF), and a third mode which is a combination of the IF and PF modes. In the IF mode, failure occurs via brittle crack propagation through the FZ, under mode I conditions (opening mode). On the other hand, in a PF scenario, failure is dominated by nugget detachment from one of the sheets (Khan, Kuntz and Zhou, 2008; Pouranvari *et al.*, 2011).

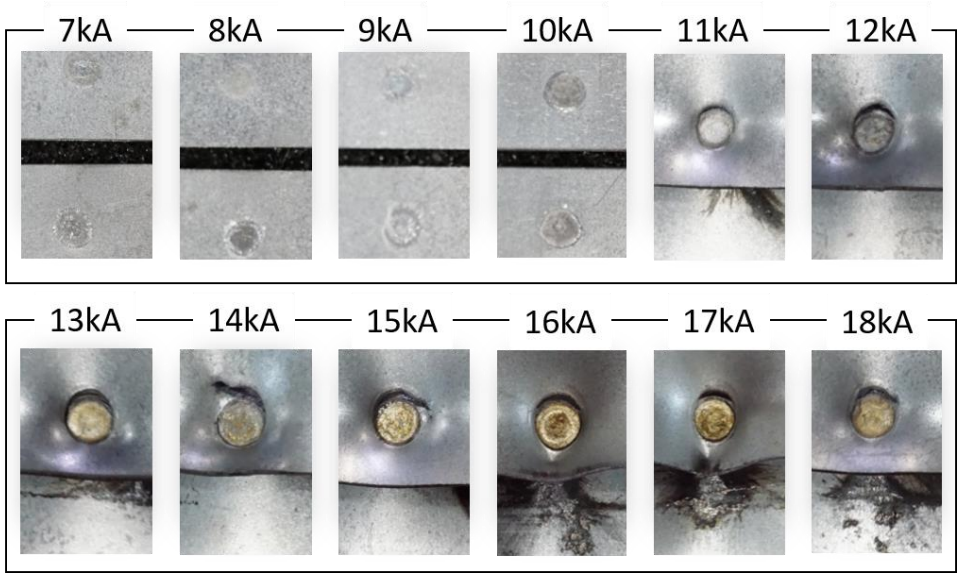

Figure 5. Failure modes obtained from tensile-shear tests under different welding currents.

Fig. 5 shows macroscopic failure modes observed after tensile-shear tests. From 7 kA to 10 kA, the welded sheets were separated at the spot weld with practically no plastic deformation, characteristic of the IF mode. This failure mode is translated into low mechanical strength and energy absorption capacity, as seen in Fig. 3 (a) and (b). Low welding currents provide a low heat input, insufficient to promote a large FZ. These unsatisfactory failure modes and mechanical behavior can be directly correlated to a small weld spot size for low welding currents, as shown in Fig. 2 and Fig. 3.

3.3 Hardness Profiles and Microstructure Analysis

A macrograph of a typical weld nugget is shown in Fig. 6. It consists of a columnar dendritic grain morphology, typical of as-cast structures. The dendritic grain structure is oriented preferentially in the thermal gradient direction (axial), normal to the solid liquid interface, towards the cooper electrodes. Fig. 7 shows the microstructure of the Base Metal (BM) and the FZ. By analyzing Fig. 7, it is possible to observe that the BM exhibits a predominant ferritic microstructure with some coarse perlite, as shown on Fig. 7 (a). On the other hand, the microstructure at the FZ exhibits a finer perlitic microstructure when compared to the BM, due to the rapid cooling involved in RSW process.

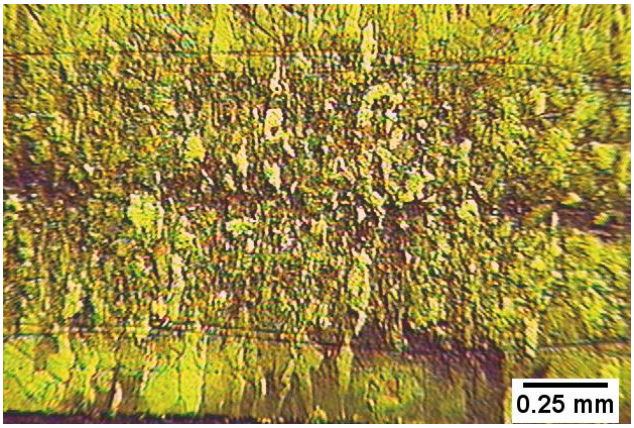

Figure 6. Macrograph of the weld nugget.

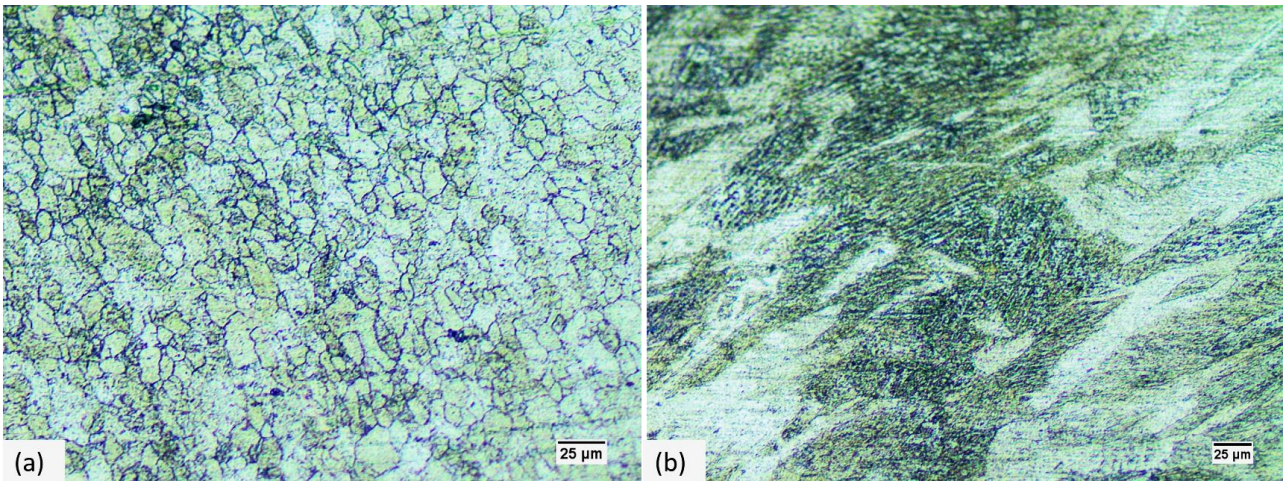

Figure 7. Microstructure at different regions: (a) Base material and (b) Fusion zone.

Hardness properties of spot welds are one of the main factors that influence their mechanical performance and failure modes. Fig. 8 shows the Vickers hardness profiles for different current levels, ranging from 12 kA to 18 kA. The hardness profiles cover three regions: BM, HAZ and FZ. It is possible to observe that the BM exhibits the lowest hardness, with values ranging between 90 and 110 $HV_{0.1}$. In contrast, the hardness values increase from the HAZ towards the FZ. The hardness values of the HAZ range from 100 to 180 $HV_{0.1}$. The average hardness of the FZ is 185 $HV_{0.1}$, with peaks of 214 $HV_{0.1}$. These results indicate that the mechanical strength of the FZ is almost twice that of the BM, and the current level has very little effect on the hardness profile.

Due to their low C and other alloy elements content, AKDQ steels are usually not susceptible to the formation of hard phases, such as martensite or bainite, even when exposed to considerably high cooling rates, associated to RSW (Alizadeh-Sh, Marashi and Pouranvari, 2014). Therefore, such increase in hardness observed in the FZ, when compared

to the BM, can be attributed to the formation of finer perlite due to the rapid cooling at the FZ and HAZ, as shown in Fig. 7 (b), which is favorable to the mechanical properties.

Chakraborty et al. observed a similar hardness profile for spot welds performed on Interstitial Free (IF) steel and attributed it to a higher dislocation density and precipitate formation during the thermal cycles (Chakraborty, Shome and Pal, 2011). Possibly, the increase in hardness observed in the FZ can attributed to both finer perlite formation and higher dislocation density promoted by the thermal cycles during the welding operations.

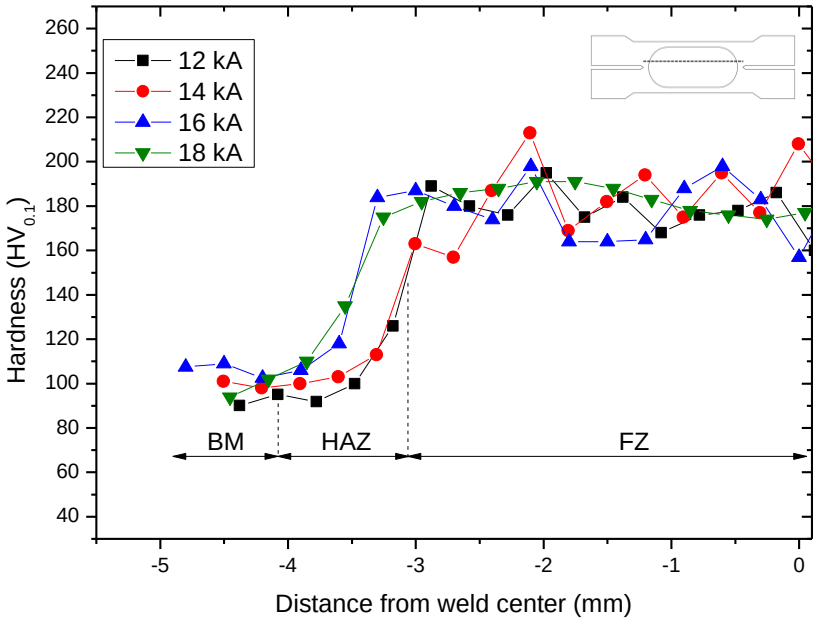

Figure 8. Vickers hardness profiles across the spot weld cross section.

4. CONCLUSIONS AND OUTLOOK

From the results obtained in this study, the following conclusions can be drawn:

(1) In a structural point-of-view, the main requirement for a spot weld is the pullout failure mode in a tensile-shear test. For the investigated material, a considerable increase in both tensile-shear load and energy absorption were observed when employing welding currents above 10 kA, which is the minimum welding current to promote an adequate spot weld size and the required pullout failure mode. Therefore, as shown in Fig. 9, the minimum recommended welding current for the investigated steel sheet is 10 kA.

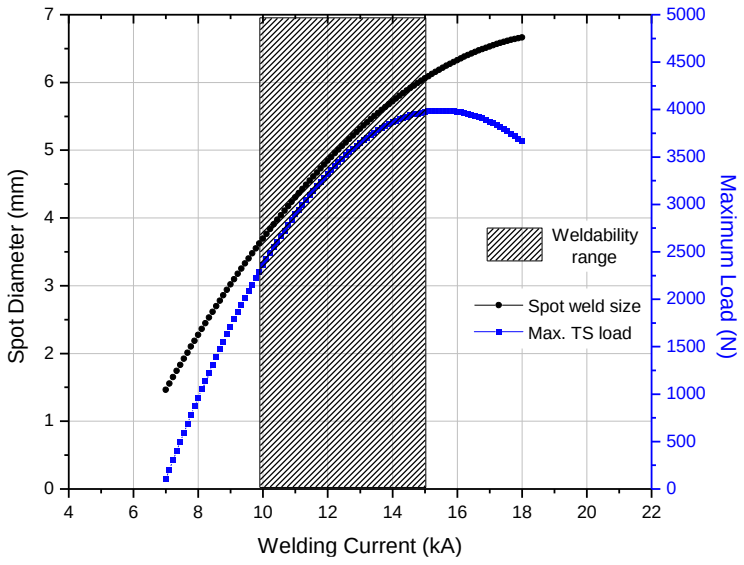

Figure 9. Weldability range.

(2) It was observed that the maximum allowable electrode indentation depth of 20%, as recommended by literature and shop floor practice, is a very conservative value, since the tensile-shear strength and energy absorption capacity, hence joint strength, can still be increased for higher weld currents. Such level of indentation was observed at 13kA.

(3) There is no considerable increase in the mechanical performance of the spot welds for welding currents above 15 kA. Additionally, when applying welding currents above 15 kA, severe molten expulsion phenomena was observed, which may impair the quality of the spot welds. Bearing this in mind, the maximum recommended welding current for the investigated steel sheet is 15 kA, as shown in Fig. 9.

5. ACKNOWLEDGEMENTS

The financial support provided by CNPq through grant 300886/2013-6 is gratefully acknowledged.

6. REFERENCES

American Welding Society, 2012. *Test methods for evaluating the resistance spot welding behavior of automotive sheet steel materials* (AWS Standard No. D8.9-12).

American Society for Testing and Materials, 2017. *Standard Test Method for Microindentation Hardness of Materials (*ASTM Standard No. E384-17).

International Organization for Standardization, 2006. *Resistance Welding - Testing of Welds - Peel and chisel testing of resistance spot and projection welds* (ISO Standard No. 10447).

Khan, M., Kuntz, M. and Zhou, Y., 2008. "Effects of weld microstructure on static and impact performance of resistance spot welded joints in advanced high strength steels". *Science and Technology of Welding and Joining,* Vol. 13, p. 294-304.

Kianersi, D. *et al.*, 2014. "Resistance spot welding joints of AISI316L austenitic stainless steel sheets: Phase transformations, mechanical properties and microstructure characterizations." *Materials and Design,* Vol. 61, p. 251-263.

Kianersi, D., Mostafaei, A. and Ali, A., 2014. "Resistance spot welding joints of AISI 316L austenitic stainless steel sheets: Phase transformations, mechanical properties and microstructure characterizations." *Materials and Design,* Vol. 61, pp. 251-263.

Kong, J. *et al.*, 2014. "Effect of boron content and welding current on the mechanical properties of electrical resistance spot welds in complex-phase steels." *Materials and Design,* Vol. 54, p. 598-609.

Liu, W. *et al.*, 2012. "The influences of nugget diameter on the mechanical properties and the failure mode of resistance spot-welded metastable austenitic stainless steel." *Materials and Design,* Vol. 33, p. 292-299.

Martín, O. *et al.*, 2014. "Assessment of resistance spot welding welding qualitgy based on ultrasonic testing and tree-based tchniques." *Journal of Materials Processing Technology,* Vol. 214, p. 2478-2487.

Pouranvari, M., Asgari, H., Mosavizadch, S. and Goodarzi, M., 2007. "Effect of weld nugget size on overload failure mode of resistance spot welds." *Science and Technology of Welding and Joining,* Vol. 12, p. 217-225.

Pouranvari, M. *et al.*, 2014. "Resistance spot welding of AISI 430 ferritic stainless steel: phase transformation and mechanical properties." *Materials and Design,* Vol. 56, p. 258-263.

Pouranvari, M. *et al*., 2011. "Influence of fusion zone size and failure mode on mechanical performance of dissimilar resistance spot welds of AISI 1008 low carbon steel and DP600 advanced high strength steel". *Materials and Design,* Vol. 32, p. 1390-1398.

Pouranvari, M. M. S., 2011. "Failure mode transition in AHSS resistance spot welds. Part I. Controlling factors." *Materials Science and Engineering A,* Vol. 528, p. 8337-8343.

Runnemalm, A. *et al*., 2014. "Inspection of Spot Welds by Thermography." *Journal of Nondestructive Evaluation,* Vol. 33, p. 398-406.

Sun, X. *et al.*, 2008. "Effects of fusion zone size and failure mode on peak load and energy absorption of advanced high strength steel spot welds under lap shear loading conditions." *Engineering Failure Analysis ,* Vol. 15, p. 356-367.

Uilj, N. J. D., 2015. *Resistance Spot Welding of Advanced High Strength Steels.* Ph.D. thesis, Delfit Technische Universiteit, Delfit.

Wan, X. *et al.*, 2014. "Modelling the effect of welding current on resistance spot welding of DP600 steel". *Journal of Materials Processing Technology,* Vol. 214, p. 2723-2729.

Zhang, Y. *et al.*, 2007. "Online quality inspection of resistance spot welded joints based on electrode indentation using servo gun." *Science and Technology of Welding and Joining,* Vol. 12, p. 449-454.

7. RESPONSIBILITY NOTICE

The authors are the only responsible for the printed material included in this paper.